ACS APPLIED MATERIALS & INTERFACES

Research Article

Cite This: ACS Appl. Mater. Interfaces 2019, 11, 4123−4130

www.acsami.org

Anisotropic Photoresponse of the Ultrathin GeSe Nanoplates Grown by Rapid Physical Vapor Deposition

Jinyang Liu,[*,†,‡,§,∥,#] Yuhan Zhou,[†,#] Yue Lin,[⊥] Mingling Li,[⊥] Hongbing Cai,[*,⊥] Yichun Liang,[†] Mengyu Liu,[†] Zhigao Huang,[†,‡,§,∥] Fachun Lai,[†,‡,§,∥] Feng Huang,[*,†,‡,§,∥] and Weifeng Zheng[†]

[†]College of Physics and Energy, Fujian Normal University, Fuzhou, 350117, P.R. China

[‡]Fujian Provincial Key Laboratory of Quantum Manipulation and New Energy Materials, Fuzhou 350117, P.R. China

[§]Fujian Provincial Collaborative Innovation Center for Optoelectronic Semiconductors and Efficient Devices, Xiamen, 361005, P.R. China

[∥]Fujian Provincial Engineering Technology Research Center of Solar Energy Conversion and Energy Storage, Fuzhou, 350117, China

[⊥]Hefei National Laboratory for Physical Science at the Microscale, University of Science and Technology of China, Hefei, Anhui 230026, P.R. China

Supporting Information

ABSTRACT: Anisotropic materials, especially two-dimensional (2D) layered materials formed by van der Waals force (vdW) with low-symmetry, have become a scientific hot-spot because their electrical, optical, and thermoelectric properties are highly polarization dependent. The 2D GeSe, a typical anisotropic-layered orthorhombic structure and narrow bandgap (1.1−1.2 eV) semiconductor, potentially meets these demands. In this report, the ultrathin elongated hexagonal GeSe nanoplates were successfully synthesized by the rapid physical vapor deposition method developed here. The ultrathin elongated hexagonal GeSe nanoplates have a zigzag edge in the long edge and an armchair edge in the short edge. In addition, the typical Raman mode exhibited 90° periodic vibration, having its maximum intensity between the zigzag direction or the zigzag and armchair direction, indicating an anisotropic electron−phonon interaction. Furthermore, the field effect transistor devices based on the elongated hexagonal GeSe nanoplates were constructed and exhibited the p-type semiconducting behavior with a high photoresponse characteriscs. Finally, the polarized sensitive photocurrent was identified, further revealing the intrinsically anisotropy of the GeSe nanoplate. The results illustrated here may give a useful guidance to synthesize the 2D-layered anisotropic nanomaterials and further advance the development of the polarized photodetector.

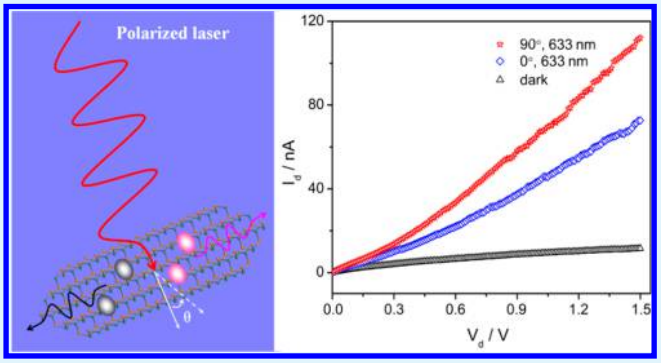

KEYWORDS: *GeSe nanoplate, rapid physical vapor deposition, two-dimensional, polarization-dependent Raman spectroscopy, anisotropic photoresponse*

INTRODUCTION

Recently, two-dimensional (2D) layered nanomaterials have attracted a great deal of interest in the nano-optoelectronic devices including photodetectors and field effect transistors (FETs)[1−3] Nowadays, graphene and graphitic structured transitional metal dichalcogenides (such as MoS_2, WS_2, $MoSe_2$, WSe_2, and so forth) are the most studied 2D layered nanomaterials, whose physicochemical properties have been well explored.[4−6] However, another group of 2D layered nanomaterials, phosphorene-like structured main group metal chalcogenides such as IV−VI (V = Ge, Sn, Pb; VI = S, Se, Te),[7−11] V−VI (V = As, Sb, Bi; VI = S, Se, Te) group compounds[12,13] have attracted more and more attention. Such materials are made up of earth abundant and environmentally friendly elements and exhibit comparable conductivity as graphitic structured 2D layered nanomaterials but with much lower structural symmetry and therefore more remarkable anisotropic feature, which would favor the polarization- or direction-dependent electrical, optical, and thermoelectric application[8,14−16]

As a typical member of these materials, GeSe, a p-type semiconductor, has gained great of interest due to its narrow bandgap (1.1−1.2 eV) that is suitable to fabricate a solar cell.[17,18] In addition, GeSe exhibits unique high-speed reversible phase transition accompanied by remarkable switching in refractive index.[19] All of the above features endow the

Received: November 4, 2018
Accepted: January 7, 2019
Published: January 7, 2019

DOI: 10.1021/acsami.8b19306
ACS Appl. Mater. Interfaces 2019, 11, 4123−4130

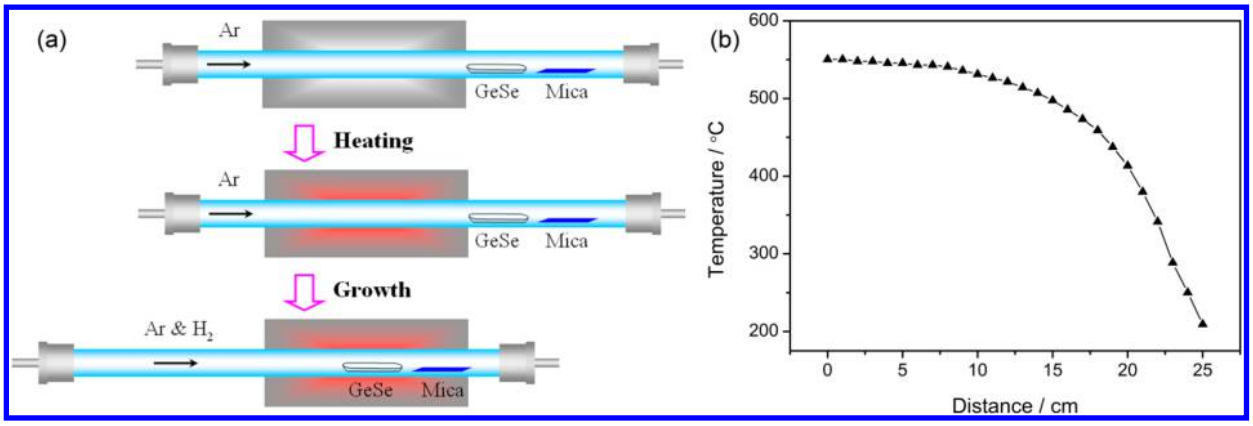

Figure 1. (a) The schematic of the typical home-built equipment with the rPVD method; (b) the temperature gradient in the furnace.

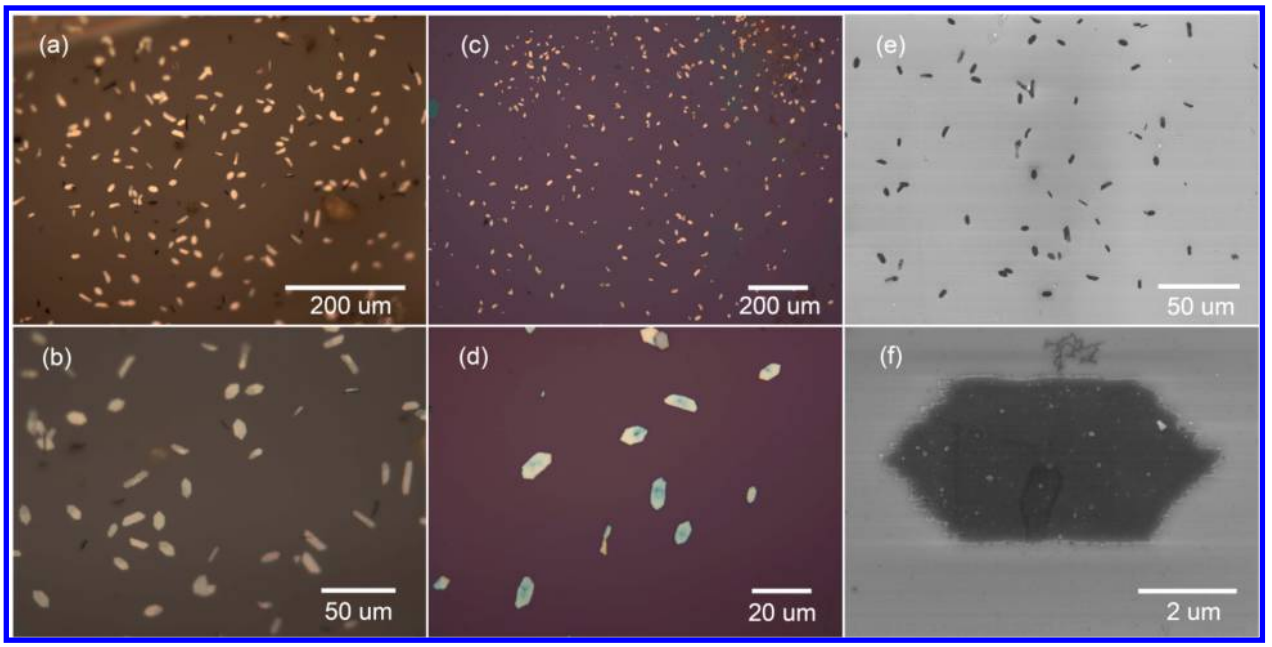

Figure 2. Morphology of the elongated hexagonal GeSe nanoplates characterized by OM and SEM (a,b) and (c,d) with OM images of the as-product on mica substrate and on SiO_2/Si substrate, respectively; SEM images (e,f) of the elongated hexagonal GeSe nanoplates on the SiO_2/Si substrate.

GeSe 2D nanomaterials with significant application in the field of photoelectrics. Thereupon, efficient preparation of these 2D nanomaterials have become an issue of great interest. For preparing such 2D nanomaterials, exfoliation is a common and universal route, which suffers from its low yield.[8] Physical/chemical "bottom-up" fabrication method would be more favorable for practical applications.[10,20] Wan et al. have reported a solution for synthesizing GeSe nanosheets with uniform elongated hexagonal shape.[17] However, these nanosheets are still too thick (about 294 nm), which might be unfavorable for exhibiting 2D size effect. Mayer et al.[21] reported a similar route and succeeded in synthesizing GeSe nanobelts with the thickness of 75 nm. Although this was a significant progress, the capping ligands that remain on the surface of 2D nanomaterials are still a disadvantage for these chemical routes. Physical vapor deposition (PVD) method is suggested to be a high efficient method for fabricating many 2D nanomaterials.[22−24] Unlike chemical routes which usually result in residual of capping ligands on the surface of product, PVD methods leave a much cleaner surface for the product and favor the investigation of optical and electrical properties. Choi et al.[25] have reported the deposition of GeSe microcombs on the Si wafer using the PVD method and studied the electrical and photoresponse property of the product. Nevertheless, it remains a great challenge to synthesize high-quality nanosized GeSe 2D materials. Moreover, as an anisotropic structured 2D nanocrystal, GeSe is in all probability exhibiting a polarized light sensitive photoresponse, while up to now there is still no investigation.[26]

In this work, uniform elongated hexagonal GeSe nanoplates have been successfully synthesized using a modified rapid physical vapor deposition (rPVD) method. The thickness of the as-prepared nanoplates is as low as 15.0 nm, which can be regarded as, so far, the thinnest GeSe nanoplates fabricated following "bottom-up" route. Moreover, the photoresponse of the product to the polarized light is also investigated in the presented work. It is found that under the irradiation of light with a different polarization direction, the as-product exhibits a distinct Raman response, which demonstrates a 4-fold symmetry. Also, because of such anisotropic electron−phonon

DOI: 10.1021/acsami.8b19306
ACS Appl. Mater. Interfaces 2019, 11, 4123−4130

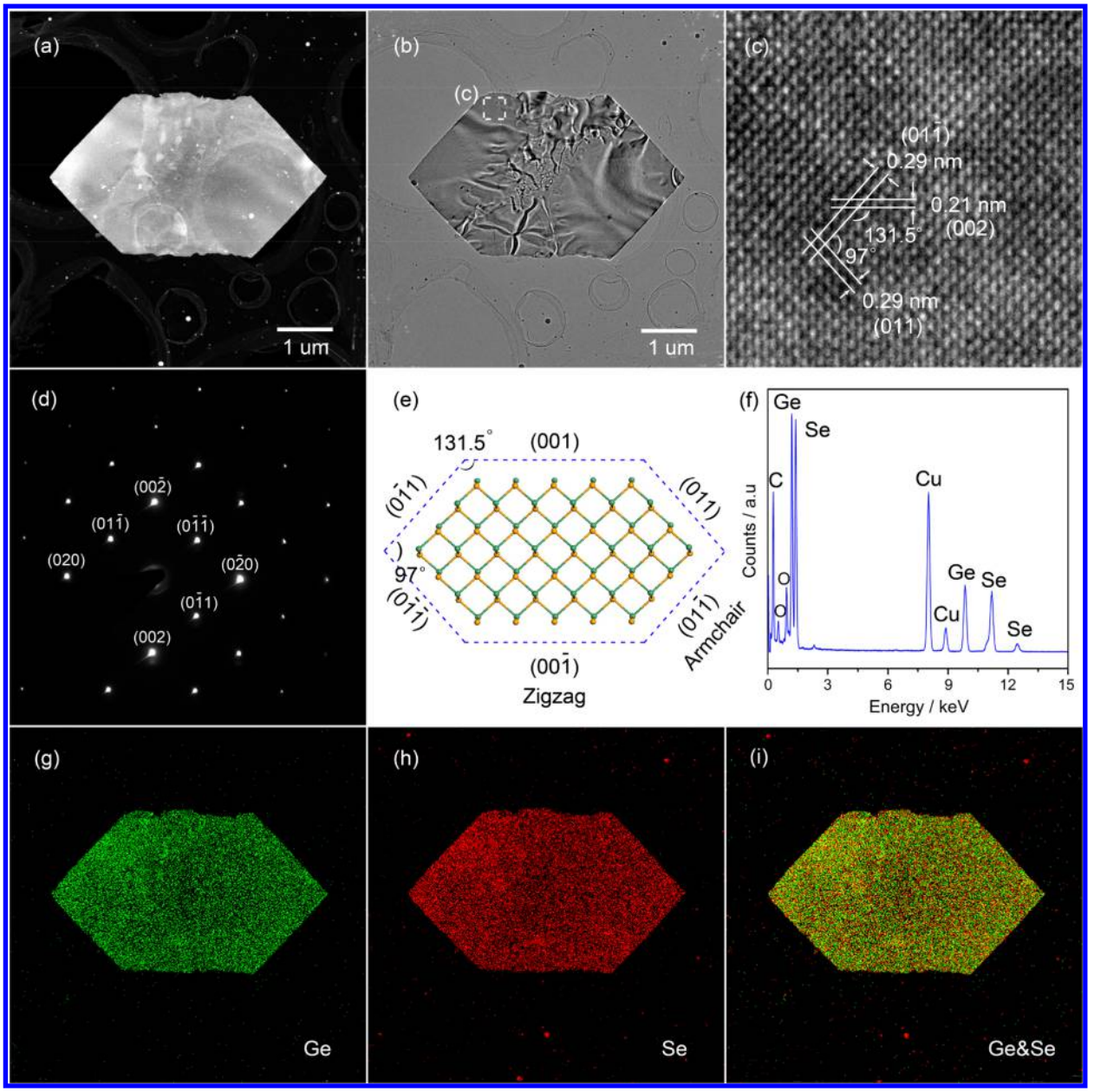

Figure 3. Crystal structure, chemical composition, and structural model of the elongated hexagonal GeSe nanoplate. (a,b) HAADF-STEM image and low-magnification TEM image of the representative elongated hexagonal GeSe plate, respectively. (c) HRTEM of the region labeled in (b). (d–f) SAED pattern, structural model, and EDX spectrum of the elongated hexagonal GeSe nanoplate, respectively. (g,h) Ge and Se element mapping image, respectively. (i) Element maps combined with Ge and Se.

interaction, the photoconduction of the elongated hexagonal GeSe nanoplate exhibits polarized light sensitive response. The work shown here may offer distinct perception on the deep understanding of the effects resulting from the anisotropic layered 2D nanostructure and is of significance for further application in the polarization-dependent photodetectors.

RESULTS AND DISCUSSION

The Figure 1 illustrated the typical home-built equipment with the rPVD method. In contrast to the conventional vapor deposition method, the rPVD developed here has some advantages including fast heating-up, nearly no quantity loss in the heating process and controllable growth temperature and time. Figure 1b shows the temperature gradient of the furnace. As demonstrated in Figure 1a, the GeSe powder worked as the reactive material was quickly inserted into the heating zone after reaching the predefined temperature. Then the GeSe powder was sublimated and transferred by Ar/H_2, and subsequently the products were successfully synthesized on the mica substrate located on the downstream from the heating zone of ~14–20 cm, where the temperature were about 508–412 °C.

As the optical microscope (OM) demonstrated in Figure 2a,b, the as-products were uniformly distributed on the mica substrate with an elongated hexagonal shape. Furthermore, it can be seen that the as-products have the platelike structure with a smooth edge. In addition, its thickness was measured to less than 15 nm (shown in Supporting Information, Figure S1a,b) by atomic force microscopy (AFM). Extensive AFM observations reveal that the average thickness of the nanoplates

DOI: 10.1021/acsami.8b19306
ACS Appl. Mater. Interfaces 2019, 11, 4123–4130

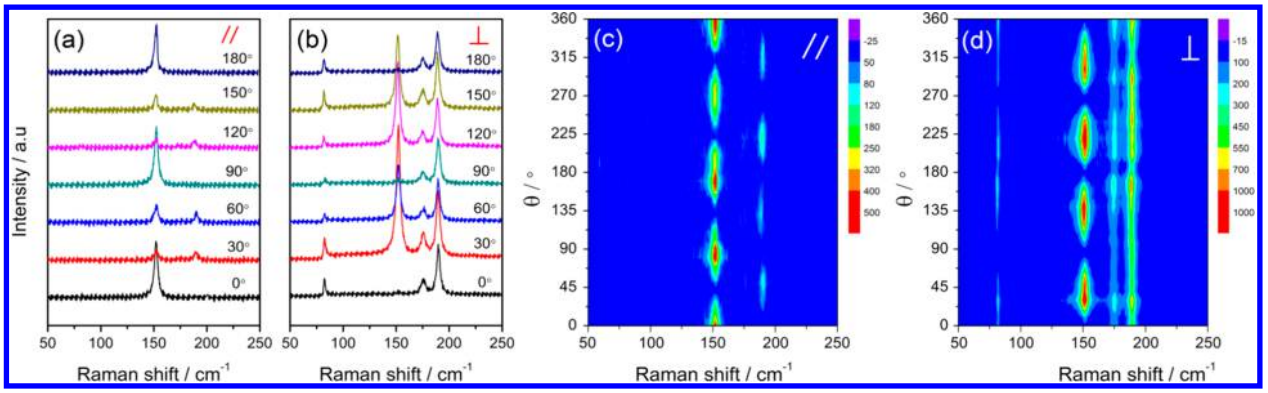

Figure 4. Polarization-dependent Raman spectroscopy of the elongated hexagonal GeSe nanoplate. Raman spectroscopy and contour color map characterized under (a,c) parallel and (b,d) perpendicular, respectively.

is ∼15 nm (shown in Supporting Information, Figure S1c), indicating that the GeSe nanoplate was about 10 layers (1 layer GeSe nanostructure is about ∼1.047 nm theoretically). This can be regarded, so far, as the thinnest record of the GeSe 2D materials attained by PVD method. To observe more clearly, the nanoplates were transferred to the SiO_2/Si (300 nm SiO_2) substrate, and OM and scanning electron microscopy (SEM) images are illustrated in Figure 2c−f. The nanoplates look very smooth and clean except some contaminate particles may be from the transferred process. The size of the products is about 4−8 μm in the long edge and 1−3 μm in the short edge. The long edge of the product is very smooth, while the short edge is a little rough as shown in the SEM image with high magnification (Figure 2f). Therefore, the GeSe nanoplates with an elongated hexagonal shape and ∼15 nm in thickness were successfully synthesized by the rPVD method.

The crystal structure and chemical composition of the as-prepared GeSe nanoplates were further characterized by transmission electron microscopy (TEM), high-magnification TEM, selected-area electron diffraction (SAED), and energy-dispersive X-ray (EDX) spectroscopy. Figure 3a is a representative high-angle annular dark-field scanning TEM (HAADF-STEM) image taken from a single nanoplate, clearly indicating the platelike structure. The diffraction contrast was observed in the bright TEM illustrated in Figure 3b, further indicating the low thickness of the elongated hexagonal GeSe nanoplate. Figure 3c demonstrated the high-resolution TEM (HRTEM) image labeled in Figure 3b. The intersection angle between the two lattice fringes (a lattice spacing of ∼0.29 nm) of ∼97° was obtained, which is well consistent with the planes of (011) and $(01\bar{1})$ of the orthorhombic GeSe crystal structure.[17] On the other hand, another lattice fringe which runs parallel to the long edge of the GeSe nanoplate had the lattice spacing of ∼0.21 nm. The intersection angle of the lattice fringes is approximately 131.5°, which is in good agreement with the angle between the planes of the (002) and $(01\bar{1})$.[17]

The SAED was used to further confirm the crystallographic orientation. Figure 3d, taken on an individual nanoplate, reveals that the product is an orthorhombic structured GeSe with the long axis of hexagonal sheet along the [002] direction, while the brachyaxis is along the [010] direction. Consequently, the exposed side of these nanoplate can be indexed to be the (100) lattice plane. Therefore, the structure model of these GeSe nanoplates was proposed (Figure 3e) based on the shape, interfacial angle, and crystal structure shown above. The ultrathin GeSe nanoplates have a zigzag edge in the long edge and an armchair edge in the short edge as shown in Figure 3e. Then, the chemical composition of the individual GeSe nanoplate was characterized by EDX spectroscopy and corresponding results were illustrated in Figure 3f−i. The Ge and Se elements were uniformly distributed on the whole nanoplate with an atomic ratio of ∼1:1. Therefore, it can be seen that the as-products are the ultrathin elongated hexagonal GeSe nanoplates with a zigzag edge in the long edge and an armchair edge in the short edge.

Raman spectroscopy is a useful technique to characterize crystal orientations and vibration symmetry. At first, the Raman spectra of the elongated hexagonal GeSe nanoplate was characterized by excited laser with different energy (532 and 633 nm) shown in Supporting Information, Figure S2. Four Raman peaks located at 81.4, 150.9, 174.5, and 188.3 cm^{-1} were observed excited by 633 nm laser. These modes are derived from A_g^3 (TO) or B_{1u} (LO), B_{3g}^1 (TO), A_g^2 (TO), or B_{2g} (LO), as well as A_g^1 (TO) (herein, LO represent longitudinal optical phonon, while TO represent transverse optical phonon), respectively, as previous reported.[27,28] However, only two modes at 150.9 and 188.3 cm^{-1} appeared excited by 532 nm laser, which are the usual phenomenon as exhibited in the previous reports.[27,28] So the 633 nm laser was chosen as the excited light in the follow experiments. Then, we further tested the Raman spectroscopy of the GeSe nanoplate with different energy by tuning the filter excited by the 633 nm laser. The results are shown in Supporting Information, Figure S3; four Raman peaks were observed and the intensity is in a reasonable level when the energy tuned to be the 5% by the filter, indicating that it is a suitable energy level.

Then, the polarization-dependent Raman spectroscopy was performed on the elongated hexagonal GeSe nanoplate to further evaluate the vibration symmetry of chemical bonds. The polarized Raman signal was collected using backscattering mode. A polarizer was located in the incident light and an analyzer was placed in the scattering light paths, respectively (shown in Supporting Information, Figure S4).[9,29] Therefore, the parallel (∥) and perpendicular (⊥) polarization would be constructed in the measurement by taking the polarizers parallel or perpendicular to each other. The polarization angle was defined as the angle between the incident light polarization direction and the long edge of the GeSe nanoplate. Figure 4a,b illustrated a series of the polarization angles of the anisotropic Raman spectrum for the as-product under the parallel or perpendicular configuration, respectively. As demonstrated,

DOI: 10.1021/acsami.8b19306
ACS Appl. Mater. Interfaces 2019, 11, 4123−4130

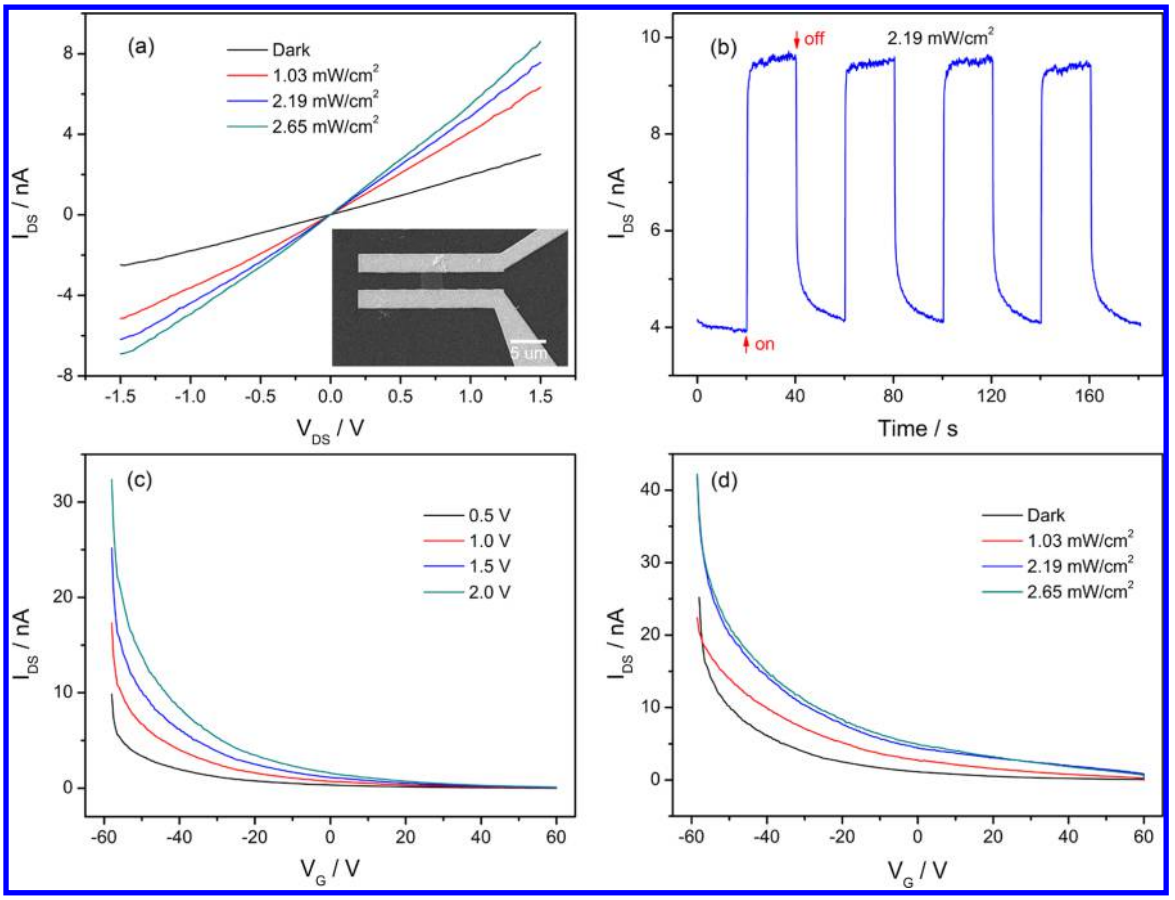

Figure 5. Electronic properties of the FET device based on the elongated hexagonal GeSe nanoplate. (a) The typical I_{DS}−V_{DS} curves performed in the dark or under the white light. Inset: SEM image of the FET device. (b) Time-resolved photoresponse at V_{DS} = 1.5 V. (c) Transfer characteristics in the different V_{DS} and (d) transfer characteristics in the different light density at V_{DS} = 1.5 V.

four peaks A_g^3 (or B_{1u}) (81.4 cm^{-1}), B_{3g}^1 (150.9 cm^{-1}), A_g^2 (or B_{2g}) (174.5 cm^{-1}), and A_g^1 (188.3 cm^{-1}) were clearly observed in the perpendicular (⊥) polarization, while only B_{3g}^1 (150.9 cm^{-1}) and A_g^1 (188.3 cm^{-1}) were observed in the parallel (∥) polarization, which are consistent with the previous reports.[27,28] Moreover, the active Raman peak intensities periodically varied with the polarization angle. This indicates the strong anisotropic Raman response of the GeSe nanoplate. This behavior can be viewed more distinctly with the contour color map for the active Raman modes, as demonstrated in Figure 4c,d. Under the parallel polarization configuration, the intensities of the B_{3g}^1 (150.9 cm^{-1}) and A_g^1 (188.3 cm^{-1}) have 90° periodic vibration. Specifically, the B_{3g}^1 mode reaches the maximum intensities at θ = 0°, 90°, 180°, or 270°, while the A_g^1 mode reaches the maximum with θ = 45°, 135°, 225°, or 315°, reversing 45°. The B_{3g}^1 (150.9 cm^{-1}) and A_g^1 (188.3 cm^{-1}) all exhibited a 4-fold anisotropy but having a different symmetry. On the basis of the crystallographic orientation analyzed by HRTEM and crystal structure model exhibited in Figure 3 of the elongated hexagonal GeSe nanoplate, it can be concluded that the maximum Raman intensity of B_{3g}^1 (150.9 cm^{-1}, ∥) appeared between the zigzag direction, while the maximum Raman intensity of A_g^1 (188.3 cm^{-1}, ∥) was observed between the zigzag and armchair direction shown in Supporting Information, Figure S5. On the other hand, under the perpendicular polarization condition in Figure 4d, the B_{3g}^1 (150.9 cm^{-1}) also has similar behavior with 90° periodic vibration. The maximum intensity located for rotation angle θ = 45°, 135°, 225°, or 315°, which indicated that the maximum Raman intensity of B_{3g}^1 (150.9 cm^{-1},⊥) was observed between the zigzag and armchair direction shown in Supporting Information, Figure S5. Although the A_g^3 (or B_{1u}) (81.4 cm^{-1}), A_g^2 (or B_{2g}) (174.5 cm^{-1}), and A_g^1 (188.3 cm^{-1}) were observed in the perpendicular polarization, the polarization-dependent Raman regularity is in disorder due to these Raman intensities being too low to be confused with the substrate signal and even not to be detected. Therefore, the GeSe nanoplates exhibited in-plane anisotropic Raman properties in which the Raman spectrum achieved the maximum intensity between the zigzag direction or the zigzag and armchair direction, indicating an anisotropic electron−phonon interaction.

The electrical properties of the elongated hexagonal GeSe nanoplates were systematically investigated using a back-gated field effect transistor (FET). The as-products were transferred to the SiO_2/p_{++} Si substrate (300 nm-thick SiO_2) at first. Then the FETs were constructed by electron beam lithography (EBL) with lift-off technology and deposited Ti/Au (10/100 nm) metal as electrodes (as shown in the inset of the Figure 5a). As is shown in the figure, two electrodes are located to the long edge of the elongated hexagonal GeSe nanoplates, which is parallel to the zigzag edge as demonstrated in Figure 3e. The typical I_{DS}−V_{DS} curves illustrated a linear relationship in the dark. It indicates the ohmic contact between the electrodes and GeSe nanoplate. Under the white light, the I_{DS}−V_{DS} curves also exhibit good linearity; the resistance (2.58 × 10^8 Ω in 1.03

DOI: 10.1021/acsami.8b19306
ACS Appl. Mater. Interfaces 2019, 11, 4123−4130

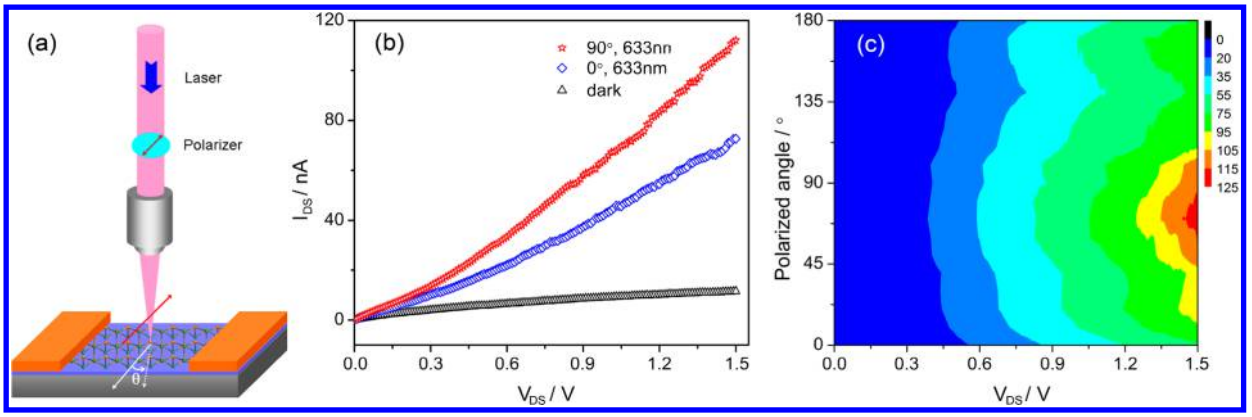

Figure 6. Angle-resolved transport of the device. (a) The schematic diagram of the equipment; (b) $I-V$ curves characterized in the dark or with 633 nm laser (the polarized angle of 0° or 90°); (c) 2D colormap of the angle-resolved transport.

mW/cm^2, 2.15 × 10^8 Ω in 2.19 mW/cm^2, 1.92 × 10^8 Ω in 2.65 mW/cm^2) decreases sharply comparing to that in the dark (5.35 × 10^8 Ω), indicating the high photoresponse. In addition, the photoresponse of the devices are related to the light intensity; namely, the photocurrents increase with light intensity increasing. As demonstrated in Figure 5b, the device exhibits excellent reversibility and stability during the measurement (2.19 mW/cm^2, V_{DS} = 1.5 V). Furthermore, the photosensitivity is extremely high. So the gain can reach as high as ∼2321% when it is defined as the ratio of the light current to the dark current, which is much higher than that reported with the similar structure.[17] The response time is less than 1 s, however, the decay time is a bit slow, which may be due to the impurities, defects at the interface between SiO_2 substrate and GeSe surface, or the interior trap states.[30] The transfer characteristics of the device illustrated in Figure 5c demonstrate that the GeSe nanoplate is the typical p-type semiconductor. The hole mobility of the device is about 0.89 cm^2 V^{-1} s^{-1} according to the formula reported,[31] which is comparable with the other 2D nanomaterials such as SnS,[32] $SnSe_2$,[33] and SnS_2[34] FETs recently. In addition, the on/off ratio is ∼500 and the result is comparable with the previous reports.[31] Furthermore, the photocurrent increases rapidly as the light intensity increases as illustrated in Figure 5d. Therefore, the FET constructed with the elongated hexagonal GeSe nanoplates exhibited the p-type semiconducting behavior with a high photoresponse characteriscs.

Besides its unique structure and Raman anisotropy, the anisotropic electrical properties of the device constructed with the elongated hexagonal GeSe nanoplate were further carried out through angle-resolved transport measurements. Figure 6a shows schematic diagram of the angle-resolved transport measurements. The polarized light is generated by the half-wave plate in light path and the focus into a small spot by optical microscope (50×, HORIBA Jobin Yvon Evolution). The polarization angle (θ) that is between the incident light polarization direction and direction that is perpendicular to the long edge of the GeSe nanoplate is tuned by a custom sample stage. The polarization direction of the 633 nm laser (34.42 nW, 210.8 mW cm^{-2}) is perpendicular to the long edge of the elongated hexagonal GeSe nanoplate where two sides are deposited Ti/Au metal as electrodes at first. The typical $I-V$ curves (Figure 6b) are nearly linear relationship, indicating that it is an ohmic contact. In addition, the current significantly increased under the 633 nm laser illumination at room temperature compared with that in the dark. Furthermore, the photoresponsivity of the device, which is defined by $R_\lambda = I_{ph}/PS$ (where $_{Iph} = I_{light} - I_{dark}$, $P \approx 210.8$ mW cm^{-2}, and $S \approx 6.79$ μm^2), and a 7.05 A W^{-1} is obtained, which is higher than that of the recently reported.[8] Besides, the specific detectivity ($D^* = R_\lambda S^{1/2}/(2eI_{dark})^{1/2}$)[32] represented the ability of a photodetector to determine weak optical signals can reach 3.04 × 10^8 Jones attributed to the ultralow dark current. Furthermore, the photocurrent is very sensitive to polarization angle, which increases 55% in 90° than that in 0° at bias voltage of 1.5 V (similar behavior are also observed with 532 nm laser illumination as shown in Supporting Information, Figure S6). So, it can be concluded that the device exhibits ultrahigh sensitivity to the 633 nm laser, especially the polarization angle. The evolution between photocurrent (Iph) and the probe polarization angle were described via the 2D colormap illustrated in Figure 6c. The photocurrent is much larger in the polarization angle around 90°, in which the polarization direction is parallel to the zigzag edge of the GeSe nanoplate (the larger photocurrent observed around 90° and 270° in one circle as illustrated in Supporting Information, Figure S7). According to the Raman spectra presented above, when the incident light polarization direction is vertical to the zigzag edge, LO phonons (B_{1u} at 81.4 cm^{-1}, and B_{2g} at 174.5 cm^{-1}) could be excited, while in the case that polarization direction is parallel to the zigzag edge only TO phonons can be excited.[27,28] It has been well-known that LO phonons exhibit relatively large scattering cross sections to the charge carriers. Therefore, the photoconductivity would be able to vary through tuning the light polarization direction, which should be the very reason for the observed polarization-dependent photoelectric response. The above results further reveal the intrinsical anisotropy of the GeSe nanoplates and application in the polarized photodetector.

CONCLUSION

The ultrathin GeSe nanoplates with an elongated hexagonal shape were successfully synthesized by the rPVD method developed here. The elongated hexagonal GeSe nanoplates have a zigzag edge in the long edge and an armchair edge in the short edge. The typical Raman mode of the ultrathin GeSe nanoplate exhibited polarization dependence. The Raman intensity reached maximum value between the zigzag direction or the zigzag and armchair direction. In addition, the FETs device based on the elongated hexagonal GeSe nanoplates were constructed and exhibited the p-type semiconducting behavior with a high photoresponse characteriscs. Besides, the

DOI: 10.1021/acsami.8b19306
ACS Appl. Mater. Interfaces 2019, 11, 4123−4130

polarized sensitive photocurrent was observed, which further reveals the intrinsically anisotropy of the GeSe nanoplate. The results illustrated here may not only provide a significance help to fabricate the 2D anisotropic materials but also further advance the polarized sensitive application.

EXPERIMENTAL SECTION

Synthesis Process. The GeSe nanoplates were synthesized using a horizontal furnace (OTF-1200X, MTI). The GeSe powder (99%, Jiangxi Ketai Advanced Materials Co. Ltd.) served as the precursors. The Figure 1a demonstrates the schematic diagram of the rPVD technique developed here. In a typical growth process, the quartz boat (0.1 g of GeSe powder) was placed on the specified location of the quartz tube, while the muscovite mica (~1 × 6 cm) was located downstream from the quartz ~14−20 cm. Before the growth, the quartz boat with the precursors was kept away from the heating center. The CVD system was cleared for several times by pumping and refilling and then heated up to 550 °C (25 min, 60 sccm Ar). After reaching the target temperature, the gas switched to 50 sccm Ar and 5 sccm H_2 and the quartz boat containing GeSe powder was moved to the heating zone and sustained for 3 min. Finally, the stove was opened until it reached room temperature. The elongated hexagonal GeSe nanoplates were transferred by using of a water ultrasonic method as previous reported.[29]

Characterization. The optical microscopy (Olympus BX51M), SEM (Hitachi SU-8010), AFM (Bruker Dimension Icon), TEM (FEI Talos, 200 kV), Raman spectroscopy (HORIBA Jobin Yvon Evolution, 532 or 633 nm) were used to characterize the elongated hexagonal GeSe nanoplates. The electron beam lithography (EBL, JEOL, JBX6300FS), sputtering deposition (Sputter-Lesker Lab18), probe station (LakeShore CRX-4K), iodine−tungsten lamp, semiconductor parameter analyzer (Keithley, 4200-SCS) were used to fabricate and characterize the FET device based on the elongated hexagonal GeSe nanoplates.

ASSOCIATED CONTENT

Supporting Information

The Supporting Information is available free of charge on the ACS Publications website at DOI: 10.1021/acsami.8b19306.

AFM image; Raman spectra with different wavelength laser or energy level; the schematic diagram of polarization-dependent Raman measurement; the relationships between maximum Raman intensity and the structure of the elongated hexagonal GeSe nanoplate; *I*−*V* curves of the device in the dark condition or under the 532 nm laser with the polarized angle of 0° and 90°; the anisotropic response in I_{pd} under the 633 nm laser described via the 2D colormap (PDF)

AUTHOR INFORMATION

Corresponding Authors

*E-mail: jyliu@fjnu.edu.cn. Tel: +86-18120795008.
*E-mail: coldice@mail.ustc.edu.cn
*E-mail: fengh@fjnu.edu.cn

ORCID

Jinyang Liu: 0000-0001-8883-4656
Yue Lin: 0000-0001-5333-511X
Hongbing Cai: 0000-0003-3186-1041

Author Contributions

#J.L. and Y.Z. contributed equally.

Notes

The authors declare no competing financial interest.

ACKNOWLEDGMENTS

This work was financially supported by the Natural Science Foundation of China (Nos. 11374052, 11504359), the Natural Science Foundation of Fujian Province of China (2017J05003), and Education Department of Fujian Province (JA15140).

REFERENCES

(1) Butler, S. Z.; Hollen, S. M.; Cao, L.; Cui, Y.; Gupta, J. A.; Gutiérrez, H. R.; Heinz, T. F.; Hong, S. S.; Huang, J.; Ismach, A. F.; Johnston-Halperin, E.; Kuno, M.; Plashnitsa, V. V.; Robinson, R. D.; Ruoff, R. S.; Salahuddin, S.; Shan, J.; Shi, L.; Spencer, M. G.; Terrones, M.; Windl, W.; Goldberger, J. E. Progress, Challenges, and Opportunities in Two-Dimensional Materials Beyond Graphene. *ACS Nano* **2013**, *7*, 2898−2926.

(2) Novoselov, K. S.; Mishchenko, A.; Carvalho, A.; Castro Neto, A. H. 2D materials and van der Waals heterostructures. *Science* **2016**, *353*, aac9439.

(3) Hu, Z. H.; Wu, Z. T.; Han, C.; He, J.; Ni, Z. H.; Chen, W. Two-dimensional transition metal dichalcogenides: interface and defect engineering. *Chem. Soc. Rev.* **2018**, *47*, 3100−3128.

(4) Roldan, R.; Chirolli, L.; Prada, E.; Silva-Guillen, J. A.; San-Jose, P.; Guinea, F. Theory of 2D crystals: graphene and beyond. *Chem. Soc. Rev.* **2017**, *46*, 4387−4399.

(5) Liu, J. Y.; Xu, Y. Y.; Cai, H. B.; Zuo, C. D.; Huang, Z. G.; Lin, L. M.; Guo, X. M.; Chen, Z. D.; Lai, F. C. Double hexagonal graphene ring synthesized using a growth-etching method. *Nanoscale* **2016**, *8*, 14178−14183.

(6) Cai, Z.; Liu, B.; Zou, X.; Cheng, H.-M. Chemical Vapor Deposition Growth and Applications of Two-Dimensional Materials and Their Heterostructures. *Chem. Rev.* **2018**, *118*, 6091.

(7) Liu, J. Y.; Huang, Q. Q.; Qian, Y. Q.; Huang, Z. G.; Lai, F. C.; Lin, L. M.; Guo, M. Z.; Zheng, W. F.; Qu, Y. Screw Dislocation-Driven Growth of the Layered Spiral-type SnSe Nanoplates. *Cryst. Growth Des.* **2016**, *16*, 2052−2056.

(8) Wang, X. T.; Li, Y. Y.; Huang, L.; Jiang, X. W.; Jiang, L.; Dong, H. L.; Wei, Z. M.; Li, J. B.; Hu, W. P. Short-Wave Near-Infrared Linear Dichroism of Two-Dimensional Germanium Selenide. *J. Am. Chem. Soc.* **2017**, *139*, 14976−14982.

(9) Yang, S. X.; Liu, Y.; Wu, M. H.; Zhao, L. D.; Lin, Z. Y.; Cheng, H. C.; Wang, Y. L.; Jiang, C. B.; Wei, S. H.; Huang, L.; Huang, Y.; Duan, X. F. Highly-anisotropic optical and electrical properties in layered SnSe. *Nano Res.* **2018**, *11*, 554−564.

(10) Ramasamy, P.; Kwak, D.; Lim, D. H.; Ra, H. S.; Lee, J. S. Solution synthesis of GeS and GeSe nanosheets for high-sensitivity photodetectors. *J. Mater. Chem. C* **2016**, *4*, 479−485.

(11) Wu, Z.; Luo, Z.; Shen, Y.; Zhao, W.; Wang, W.; Nan, H.; Guo, X.; Sun, L.; Wang, X.; You, Y.; Ni, Z. Defects as a factor limiting carrier mobility in WSe2: A spectroscopic investigation. *Nano Res.* **2016**, *9*, 3622−3631.

(12) Song, H.; et al. Highly Anisotropic Sb2Se3 Nanosheets: Gentle Exfoliation from the Bulk Precursors Possessing 1D Crystal Structure. *Adv. Mater.* **2017**, *29*, 1700441.

(13) Zhuang, A.; Li, J.-J.; Wang, Y.-C.; Wen, X.; Lin, Y.; Xiang, B.; Wang, X.; Zeng, J. Screw-Dislocation-Driven Bidirectional Spiral Growth of Bi2Se3 Nanoplates. *Angew. Chem., Int. Ed.* **2014**, *53*, 6425−6429.

(14) Yang, Y.; Liu, S.-C.; Yang, W.; Li, Z.; Wang, Y.; Wang, X.; Zhang, S.; Zhang, Y.; Long, M.; Zhang, G.; Xue, D.-J.; Hu, J.-S.; Wan, L.-J. Air-Stable In-Plane Anisotropic GeSe2 for Highly Polarization-Sensitive Photodetection in Short Wave Region. *J. Am. Chem. Soc.* **2018**, *140*, 4150−4156.

(15) Liu, B.; et al. Black Arsenic−Phosphorus: Layered Anisotropic Infrared Semiconductors with Highly Tunable Compositions and Properties. *Adv. Mater.* **2015**, *27*, 4423−4429.

(16) Arora, A.; Noky, J.; Drüppel, M.; Jariwala, B.; Deilmann, T.; Schneider, R.; Schmidt, R.; Del Pozo-Zamudio, O.; Stiehm, T.; Bhattacharya, A.; Krüger, P.; Michaelis de Vasconcellos, S.; Rohlfing,

DOI: 10.1021/acsami.8b19306
ACS Appl. Mater. Interfaces 2019, 11, 4123−4130

M.; Bratschitsch, R. Highly Anisotropic in-Plane Excitons in Atomically Thin and Bulklike 1T′-ReSe2. *Nano Lett.* **2017**, *17*, 3202−3207.
(17) Xue, D. J.; Tan, J. H.; Hu, J. S.; Hu, W. P.; Guo, Y. G.; Wan, L. J. Anisotropic Photoresponse Properties of Single Micrometer-Sized GeSe Nanosheet. *Adv. Mater.* **2012**, *24*, 4528−4533.
(18) Xue, D. J.; Liu, S. C.; Dai, C. M.; Chen, S. Y.; He, C.; Zhao, L.; Hu, J. S.; Wan, L. J. GeSe Thin-Film Solar Cells Fabricated by Self-Regulated Rapid Thermal Sublimation. *J. Am. Chem. Soc.* **2017**, *139*, 958−965.
(19) Soref, R.; Hendrickson, J.; Liang, H.; Majumdar, A.; Mu, J.; Li, X.; Huang, W.-P. Electro-optical switching at 1550 nm using a two-state GeSe phase-change layer. *Opt. Express* **2015**, *23*, 1536−1546.
(20) Vaughn, D. D.; Patel, R. J.; Hickner, M. A.; Schaak, R. E. Single-Crystal Colloidal Nanosheets of GeS and GeSe. *J. Am. Chem. Soc.* **2010**, *132*, 15170−15172.
(21) Vaughn, D. D.; Sun, D.; Levin, S. M.; Biacchi, A. J.; Mayer, T. S.; Schaak, R. E. Colloidal Synthesis and Electrical Properties of GeSe Nanobelts. *Chem. Mater.* **2012**, *24*, 3643−3649.
(22) Liu, J. Y.; Zhou, Y. H.; Liang, Y. C.; Liu, M. Y.; Huang, Z. G.; Lin, L. M.; Zheng, W. F.; Lai, F. C. Large scale SnSe pyramid structure grown by gradient vapor deposition method. *CrystEngComm* **2018**, *20*, 1037−1041.
(23) Zhao, S. L.; Wang, H. A.; Zhou, Y.; Liao, L.; Jiang, Y.; Yang, X.; Chen, G. C.; Lin, M.; Wang, Y.; Peng, H. L.; Liu, Z. F. Controlled synthesis of single-crystal SnSe nanoplates. *Nano Res.* **2015**, *8*, 288−295.
(24) Lin, M.; Wu, D.; Zhou, Y.; Huang, W.; Jiang, W.; Zheng, W. S.; Zhao, S. L.; Jin, C. H.; Guo, Y. F.; Peng, H. L.; Liu, Z. F. Controlled Growth of Atomically Thin In2Se3 Flakes by van der Waals Epitaxy. *J. Am. Chem. Soc.* **2013**, *135*, 13274−13277.
(25) Yoon, S. M.; Song, H. J.; Choi, H. C. p-Type Semiconducting GeSe Combs by a Vaporization-Condensation-Recrystallization (VCR) Process. *Adv. Mater.* **2010**, *22*, 2164−2167.
(26) Sharma, A.; Yan, H.; Zhang, L.; Sun, X.; Liu, B.; Lu, Y. Highly Enhanced Many-Body Interactions in Anisotropic 2D Semiconductors. *Acc. Chem. Res.* **2018**, *51*, 1164−1173.
(27) Zhang, X.; Tan, Q.-H.; Wu, J.-B.; Shi, W.; Tan, P.-H. Review on the Raman spectroscopy of different types of layered materials. *Nanoscale* **2016**, *8*, 6435−6450.
(28) Chandrasekhar, H. R.; Zwick, U. Raman scattering and infrared reflectivity in GeSe. *Solid State Commun.* **1976**, *18*, 1509−1513.
(29) Li, M. L.; Wu, Y. M.; Li, T. S.; Chen, Y. L.; Ding, H. Y.; Lin, Y.; Pan, N.; Wang, X. P. Revealing anisotropy and thickness dependence of Raman spectra for SnS flakes. *RSC Adv.* **2017**, *7*, 48759−48765.
(30) Hu, P.; Wen, Z.; Wang, L.; Tan, P.; Xiao, K. Synthesis of Few-Layer GaSe Nanosheets for High Performance Photodetectors. *ACS Nano* **2012**, *6*, 5988−5994.
(31) Zhou, X.; Hu, X.; Jin, B.; Yu, J.; Liu, K.; Li, H.; Zhai, T. Highly Anisotropic GeSe Nanosheets for Phototransistors with Ultrahigh Photoresponsivity. *Advanced Science* **2018**, *5*, 1800478.
(32) Li, M. L.; Zhu, Y. S.; Li, T. S.; Lin, Y.; Cai, H. B.; Li, S. J.; Ding, H. Y.; Pan, N.; Wang, X. P. One-step CVD fabrication and optoelectronic properties of SnS2/SnS vertical heterostructures. *Inorg. Chem. Front.* **2018**, *5*, 1828−1835.
(33) Zhou, X.; Gan, L.; Tian, W.; Zhang, Q.; Jin, S.; Li, H.; Bando, Y.; Golberg, D.; Zhai, T. Ultrathin SnSe2 Flakes Grown by Chemical Vapor Deposition for High-Performance Photodetectors. *Adv. Mater.* **2015**, *27*, 8035−8041.
(34) Li, B.; Xing, T.; Zhong, M.; Huang, L.; Lei, N.; Zhang, J.; Li, J.; Wei, Z. A two- dimensional Fe-doped SnS2 magnetic semiconductor. *Nat. Commun.* **2017**, *8*, 1958.

DOI: 10.1021/acsami.8b19306
ACS Appl. Mater. Interfaces 2019, 11, 4123−4130